DEUTSCHES ELEKTRONEN-SYNCHROTRON DESY

DESY 78/54
October 1978

First Observation of Photon-Photon Interactions at DORIS

by

H. J. Besch, H. W. Eisermann, B. Löhr, G. Nöldeke, M. Tonutti,
W. Vollrath, R. Wilcke
Universität Bonn

H. Hoffmann
CERN Geneva

H. C. Dehne, H. Kowalski
Deutsches Elektronen-Synchrotron DESY, Hamburg

H. J. von Eyß, H. von der Schmitt
Universität Mainz

NOTKESTRASSE 85 · 2 HAMBURG 52

First Observation of Photon-Photon Interactions at DORIS*

Abstract:

With a forward tagging system and the BONANZA detector we observed 24 $e^+e^- \rightarrow e^+e^-e^+e^-$ events but no $e^+e^- \rightarrow e^+e^-$ + hadrons. We present an upper limit for the partial width $\Gamma_{\eta' \rightarrow \gamma\gamma}$ of 11.5 keV (95% CL) which is evidence against the Han-Nambu quark model.

* Work supported by the Bundesminister für Forschung und Technologie, Germany

H.J. Besch, H.W. Eisermann, B. Löhr
G. Nöldeke, M. Tonutti+), W. Vollrath
R. Wilcke

Physikalisches Institut
der Universität Bonn

H. Hoffmann

CERN, Genève

H.C. Dehne, H. Kowalski

DESY, Hamburg

H.J. von Eyß++), H. von der Schmitt

Institut für Kernphysik
der Universität Mainz

+) now at SLAC, Stanford
++) now at Institut für Reaktorsicherheit, Köln

The investigation of photon-photon interactions (Fig. 1) at e^+e^--storage rings was suggested quite early [1]. First experimental observations of these processes were reported from Novosibirsk [2] and, using the tagging technique, from Frascati [3]. We present here results from the measurements of photon-photon interactions at the storage ring DORIS. The experiment was performed using a tagging system to detect the forward going electrons and positrons, and the BONANZA detector for the products of the $\gamma\gamma$-interaction. A general view of the central detector is given in Fig. 2. Its innermost part consists of a 5 cylinder proportional chamber system with a two-dimensional readout, followed by 3 rings of scintillators. All counters are equipped with phototubes at both ends, so accurate time and position measurements were possible. The detector was originally designed to detect antineutrons and antiprotons by their annihilation in the second ring, which is therefore 20 cm thick. The deposited energy in these annihilation counters was measured. The bunch crossing times were derived from the DORIS R.F. This arrangement of counters, in combination with one radiation length of lead after the third proportional chamber, is well suited for discriminating electrons and photons from other particles. A more detailed description of the detector is given in Ref. 4.
The DORIS tagging system (Fig. 3) is based on the fact that because of the vertical crossing angle, the beams pass through the large quadrupoles WQ1 and WQ2 off center. So these quadrupoles, together with the homogeneous septum magnet VS, are used as a magnetic spectrometer [10]. Data for the field parameters were available from the automatic bookkeeping system of DORIS. The electrons and positrons were each detected by a shower counter (e-counter), mounted in the beam pipe 12 m downstream from the interaction point, about 6 x 8 cm^2 and 10 radiation lengths thick. The shower counter provided us with energy and time information. A similar counter (γ-counter) was used to veto beam-gas Bremsstrahlung events.

The counting rates of the tagging counters were - depending on the residual gas pressure and the current in the machine - between 14 and 23 kHz (600 MeV threshold) for positrons and between 76 and 180 kHz (250 MeV threshold) for electrons.
To determine the acceptance of the tagging system we performed a Monte-Carlo calculation. The angular distribution has a very sharp peak in the forward direction and was calculated in the equivalent photon approximation [6]. The track following through the magnet system was done using a Runge-Kutta method. We found that electrons or positrons with 73% - 82% of beam momentum and up to 10 milliradians scattering angle were detected [8]. The luminosity was measured in the usual way by small angle Bhabha scattering [9].

The trigger was derived from the BONANZA detector only and required either: -

- a deposited energy of 84 MeV, i.e. twice the minimum ionization, in one of the annihilation counters, together with either a coincidence in an opposite lying counter, or ≥ 2 central charged tracks in the proportional chambers;

or: -

- ≥ 3 central charged tracks, depositing at least 20 MeV in the annihilation counters.

For the purpose of the experiment reported here this trigger, which had been optimized for another experiment [4], was sensitive mainly to electrons and photons.

If one of the above conditions was fulfilled, the information of both the central detector and the tagging system was recorded on tape.

We took data at beam energies of 2.1, 2.24 and 2.6 GeV and accumulated a total integrated luminosity of 1457 nb^{-1}. We recorded 4.6 Million triggers which reduced to 2.2 Million after rejection of obvious cosmic ray events. Among them were 54000 single tagged events, i.e. coincidences of the central detector with one tagging counter, and 214 double tagged events where both tagging counters had been hit.

The time information from the central and tagging detectors allowed us to determine the interaction time differences, i.e. the time differences between the photon emission of a tagged electron or positron and the bunch crossing immediately before the central detector event. The resolution for this time difference was 0.7 nsec FWHM. Fig. 4 shows the distribution for the single tagged event sample. The central peak contains the genuine events, a large number of beam-gas events, and some accidental background. Due to the bunch structure of DORIS, this accidental background has peaks with a separation of 8 nsec. The slightly enlarged peak at -8 nsec is caused by beam-gas events with very slow reaction particles which were therefore assigned to the next bunch crossing.

After rejecting events incorrect by more than 1 nsec and requiring at least 1 GeV deposited energy in the tagging counter 11000 events remain. Most of these events come from electroproduction off the gas molecules in the beam pipe and have consequently the correct timing. Because of this serious background we searched in this sample for events of the type

$$e^+e^- \rightarrow e^+e^-e^+e^-$$

only.
We therefore looked for events which had two nearly collinear tracks in the x,y projection (see Fig. 2), at least one of them satisfying shower conditions in the annihilation counters. From the 11000 events above, 31 satisfy this requirement. The distribution of these events along the beam is shown in Fig. 5. The peak in the interaction region contains 29 events above a small background of 0.4 ± 0.2 events. The application of the same conditions to the neighbouring bunches from Fig. 4, showed that these 29 events contain an additional background of 4.8 ± 1 events from accidental coincidences. These are all large angle e^+e^- pairs from Bhabha scattering and their number is in good agreement with the calculated accidental coincidence rate. So 24 genuine $e^+e^- \rightarrow e^+e^-e^+e^-$ events with one tagged electron or positron were measured with an error of $\pm$ 5.8 events.

The electron and positron interaction time differences of the 214 double tagged events are plotted against each other in Fig. 6.

A double periodic structure with 8 nsec period (i.e. bunch separation) can be seen. The 'cross' consists mainly of electro-production events on the residual gas with an accidental coincidence in the other tagging counter. All genuine $\gamma\gamma$-events should have both interaction time differences smaller than 1 nsec. Only 10 events satisfy this condition. The background due to electro-production estimated from the plot in Fig. 6 is 4.5 events. The background from other sources is negligible. From the 10 events lying in the time interval, only 3 do not come from the interaction region. This is in agreement with the background estimation. Thus, in the case of double tagged events, only the time coincidence condition is required to yield a fairly clean sample of $\gamma\gamma$ events.

The 7 events coming from the interaction region are all two-prongs which are nearly collinear in the x,y projection and show a shower in at least one track. So we conclude that all 7 double tagged events we observed, are due to the fourth order QED reaction $e^+e^- \rightarrow e^+e^-e^+e^-$.

The detection probability for large angle e^+e^- pairs in the BONANZA detector was calculated, using a comprehensive Monte Carlo shower program [4,5,8] . This program was tested by measuring and calculating large angle Bhabha and $e^+e^- \rightarrow \gamma\gamma$ events at energies of about 3.1 and 4.2 GeV. Good agreement within 10% was found. The QED cross section was computed in the Weizsäcker-Williams approximation [6]. A summary of the luminosities, acceptances and measured and calculated QED event rates, is given in table 1.

The QED results are in good agreement with our measurements for both single and double tagged events. In the case of double tagged events we also know that we have not recorded any $\gamma\gamma$-event with hadrons in the final state.

Our trigger was sensitive to hadronic final states containing either many charged particles or at least one photon. The η' decays mainly to such final states and its mass is well covered by our

$\gamma\gamma$-CMS energy window. Therefore it should be seen in our apparatus. The trigger probability for the η' in the central detector has been calculated with our Monte-Carlo program [5] and was found to be $14.2 \pm 1\%$ and only slightly dependent on the beam energy. The crucial parts of this computation were also performed with the EGS-program [14] and led to the same results.

The fact that we observe no η' event in the double tagged event sample leads to a new upper limit [15] for its $\gamma\gamma$-decay width:

$$\Gamma_{\eta'\to\gamma\gamma} < 11.5 \text{ keV with 95\% confidence level.}$$

As pointed out in Ref. [7], the $\gamma\gamma$-width of the η' meson is particularly sensitive to the quark charge assignment. For the fractionally charged (Gell-Mann) and the integer charged (Han-Nambu) quarks this width is

$$\Gamma^{\text{HAN NAMBU}}_{\eta'\to\gamma\gamma} = 25.6 \text{ keV} \qquad \Gamma^{\text{GELL MANN}}_{\eta'\to\gamma\gamma} = 6 \text{ keV}.$$

The big difference between them is mainly caused by the properties of the SU(3) singlet amplitude which dominates η'. The SU(3) octet amplitude leads to no differences between both models as in the π^0-case. Since the new analyses of pseudoscalar meson decays [11,12,13] confirm the SU(3) singlet dominance of η'(958) we conclude that our upper limit is evidence against the Han-Nambu quark model[16].

We acknowledge the help of many colleagues. We especially thank the DORIS crew for their cooperation and Prof. W. Paul for his continued support. We also thank Prof. P. Waloschek for drawing our attention to the tagging system of DORIS.

References:

[1] F. Low: Phys. Rev. 120 (1960) 582
[2] V.E. Balakin et al: Phys. Lett. 34B (1971) 663
[3] C. Bacci et al: Lett. Nuovo Cim. 3 (1972) 709
[4] H.-J. Besch et al: Phys. Lett., to be published; Bonn-HE-77/15
[5] H. von der Schmitt: Thesis, Mainz (1978)
[6] S.Brodsky, T.Kinoshita, H.Terazawa: Phys. Rev. D4 (1971) 1532
[7] H.Suura, T.F.Walsh, B.L.Young: Lett. Nuovo Cim. 4 (1972) 505
[8] H.W. Eisermann: Thesis, Bonn (1978)
[9] G. Barbiellini et al: Atti Accad. Naz. Lincei 44(1968) 223
[10] P. Waloschek: J. Physique 35 Suppl. 3 (1974) C2-35; DESY 73/57
[11] A. Bramon, M. Greco: Phys. Lett. 48B (1974) 137
[12] F.D. Gault et al: Nuovo Cim. 24A (1974) 259
[13] A. Kazi et al: Lett. Nuovo Cim. 15 (1976) 120
[14] EGS: The HEPL-SLAC-Monte Carlo Electron Gamma Shower Program; see: R.L. Ford, W.R. Nelson: SLAC Report No. 210 (1978)
[15] L. Paoluzi et al: Lett. Nuovo Cim. 10 (1974) 435
[16] We note that this upper limit combined with the measured branching ratio $\Gamma_{\gamma\gamma}/\Gamma_{tot}$ (P. Dalpiaz et al: Phys. Lett. 42B (1972) 377) gives an independent but somewhat larger upper limit for the η'-width (A. Duane et al: Phys. Rev. Lett. 32 (1974) 425)

Figure captions:

Fig. 1: $\gamma\gamma$-interaction

Fig. 2: BONANZA detector

Fig. 3: The tagging system of DORIS showing particle trajectories (note the different horizontal and vertical scales)

Fig. 4: Interaction time difference distribution for all single tagged events (shower counter threshold 1 GeV)

Fig. 5: z-distribution for the single tagged collinear events showing at least one showering track

Fig. 6: Two-dimensional interaction time difference distribution for the double tagged events

beam energy [GeV]		2.1	2.24	2.6
tagged $\gamma\gamma$-CMS-energy [GeV]		.76-1.13	.81-1.21	.94-1.4o
luminosity $\int L\,dt$ $[nb^{-1}]$		242	499	716
acceptance for events satisfying the geometrical constraints of the central and tagging detector	$e^+e^- \rightarrow e^+e^-e^+e^-$ double tag	73%	80%	81%
	$e^+e^- \rightarrow e^+e^-e^+e^-$ single tag	41%	47%	49%
QED cross-sections in the geometrical acceptance of the central and tagging detector	$e^+e^- \rightarrow e^+e^-e^+e^-$ double tag	5.2 pb	4.7 pb	3.8 pb
	$e^+e^- \rightarrow e^+e^-e^+e^-$ single tag	34.o pb	3o.1 pb	24.4 pb
expected number of events	$e^+e^- \rightarrow e^+e^-e^+e^-$ double tag	5		
	$e^+e^- \rightarrow e^+e^-e^+e^-$ single tag	18.9		
observed number of events	$e^+e^- \rightarrow e^+e^-e^+e^-$ double tag	7 ± 2.7		
	$e^+e^- \rightarrow e^+e^-e^+e^-$ single tag	24 ± 5.8		

The lower acceptance of the single tag events is caused by more restrictive conditions for the selection of these events.

Table 1

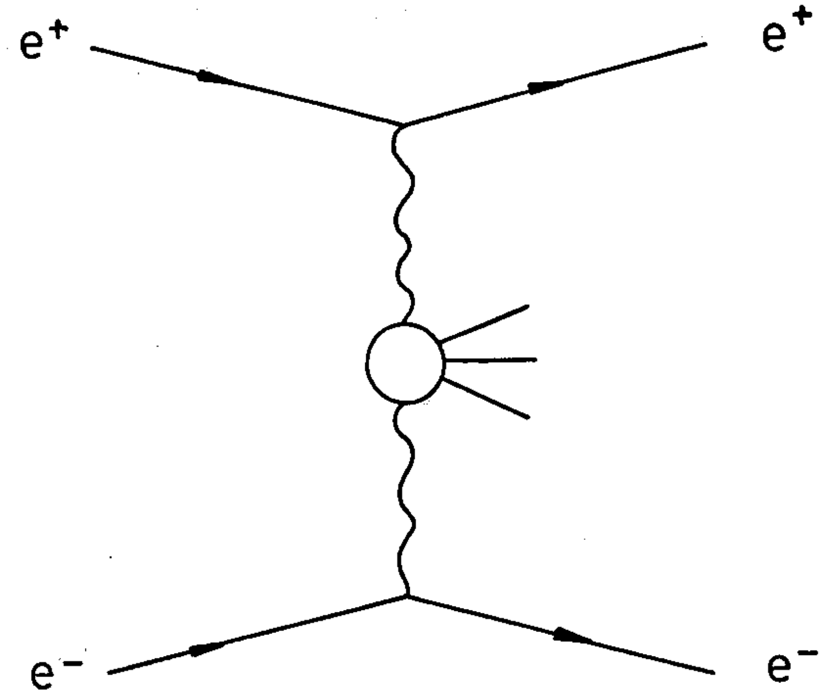

Fig.1

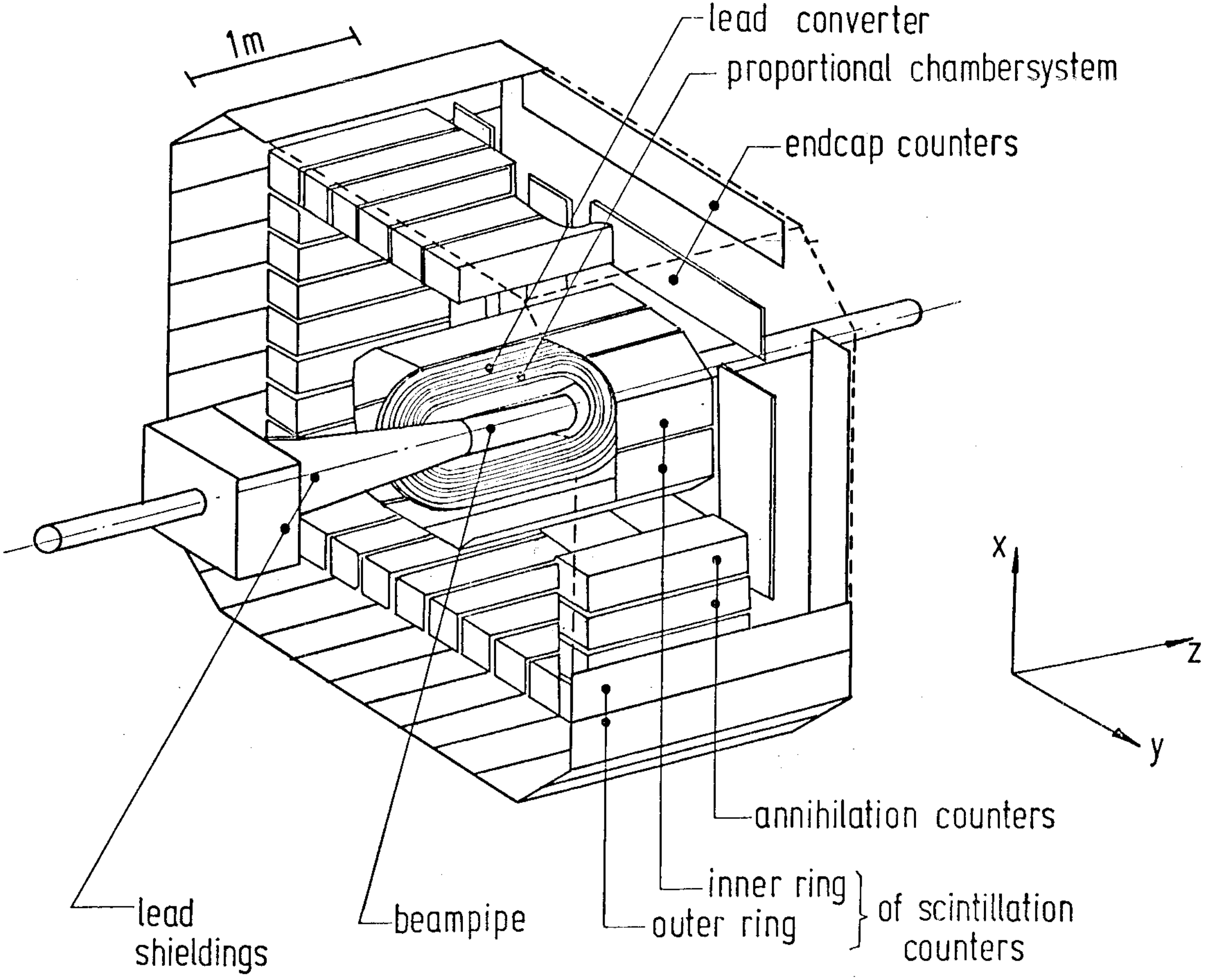
1m
lead converter
proportional chambersystem
endcap counters
x
z
y
annihilation counters
inner ring
outer ring
of scintillation counters
lead shieldings
beampipe

Fig. 2

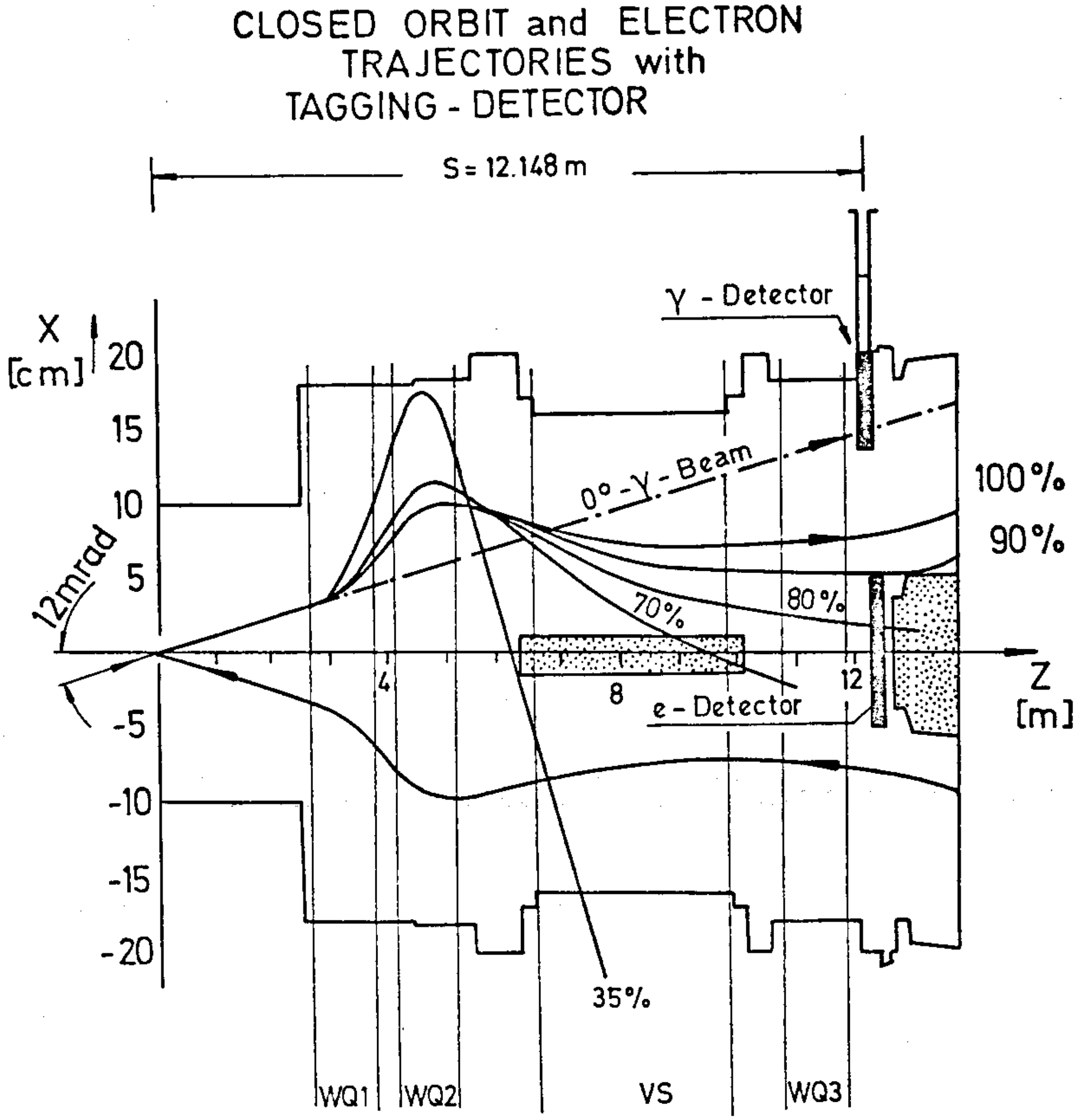
CLOSED ORBIT and ELECTRON
TRAJECTORIES with
TAGGING - DETECTOR
S = 12.148 m
γ - Detector
X
[cm]
20
15
10
5
-5
-10
-15
-20
12mrad
0° - γ - Beam
100%
90%
80%
70%
4
8
12
Z
[m]
e - Detector
35%
WQ1
WQ2
VS
WQ3

Fig. 3

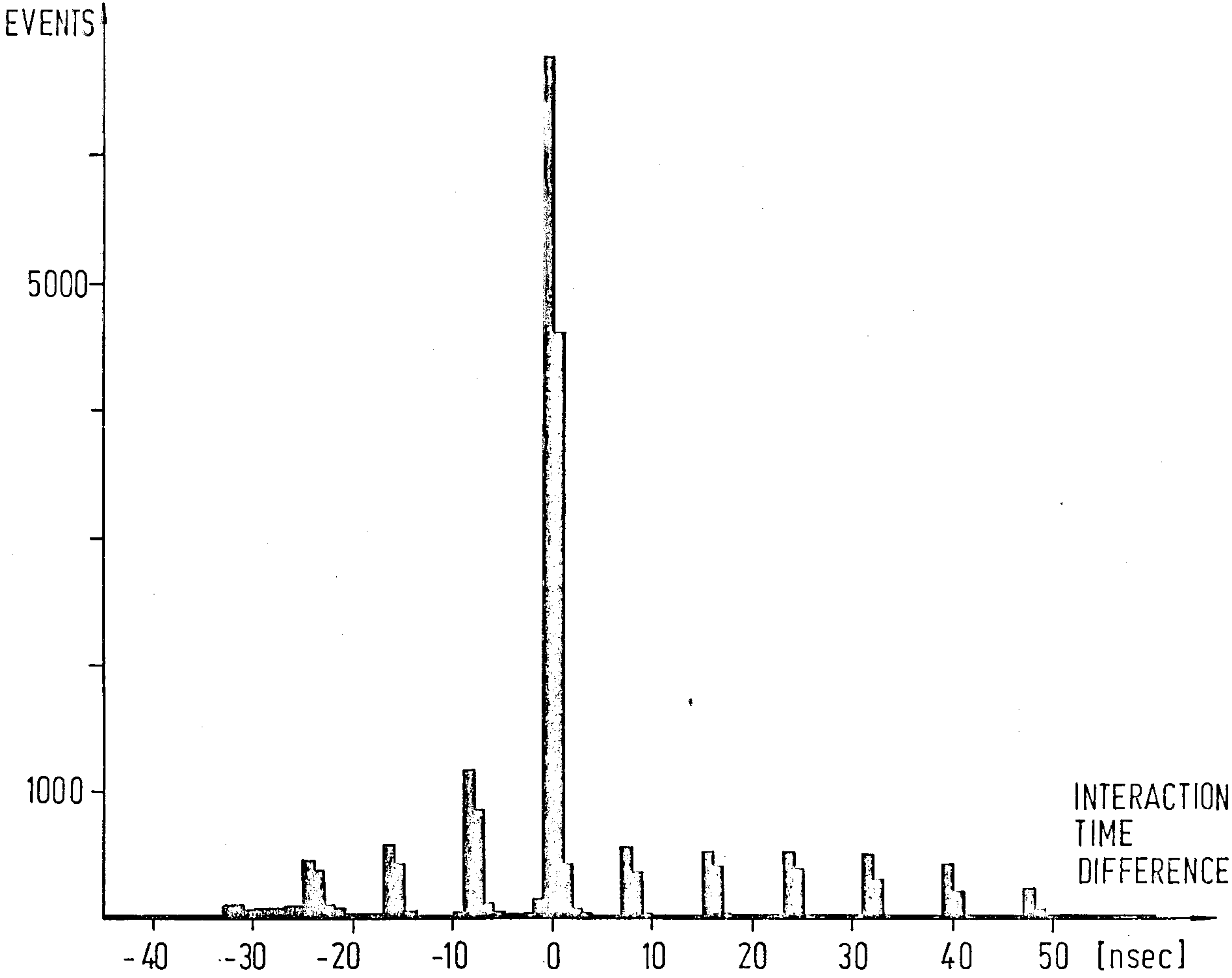
EVENTS
5000
1000
INTERACTION
TIME
DIFFERENCE
-40
-30
-20
-10
0
10
20
30
40
50
[nsec]

Fig. 4

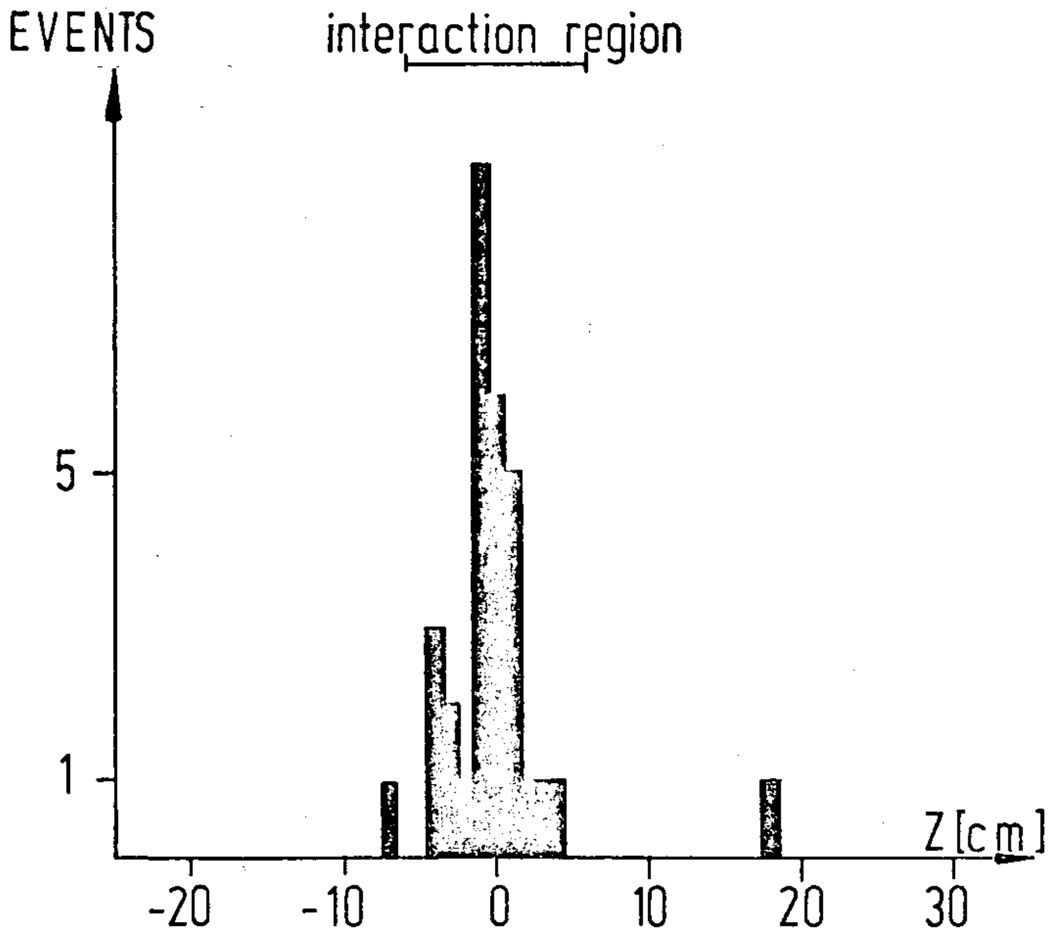

FIG. 5

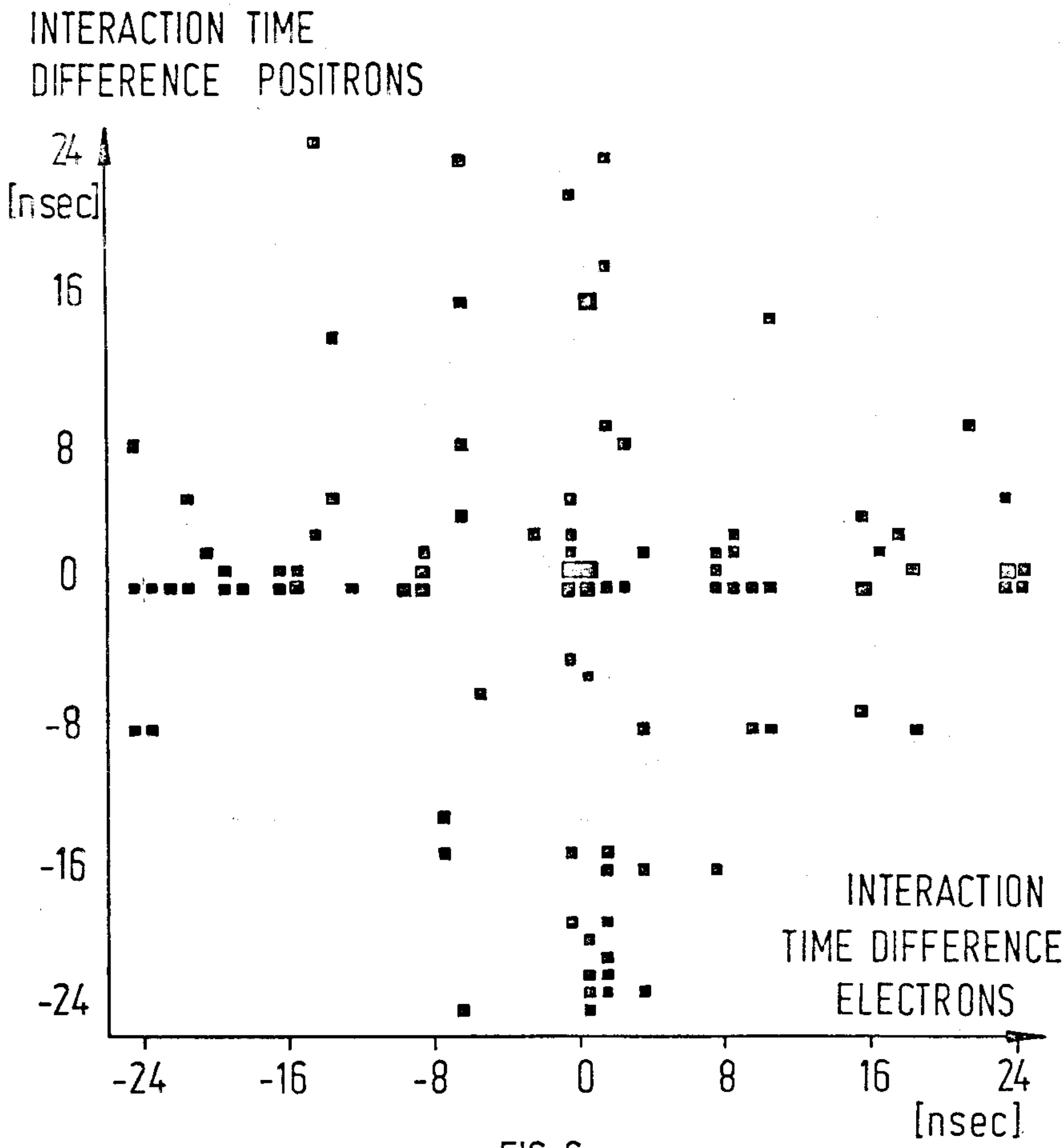
INTERACTION TIME
DIFFERENCE POSITRONS
24
[nsec]
16
8
0
-8
-16
-24
INTERACTION
TIME DIFFERENCE
ELECTRONS
-24
-16
-8
0
8
16
24
[nsec]

FIG. 6